20

Analysis of the general structure of the E–I characteristic of high current superconductors with particular reference to a Nb–Ti SRM wire

D.P. Hampshire* and H. Jones

The Clarendon Laboratory, Parks Road, Oxford OX1 3PU, UK

Received 7 January 1987; revised 1 June 1987

In this Paper the compatability between a three parameter fit, which assumes a normal density distribution of critical currents, and the familiar empirical two parameter law ($V = \alpha I^n$) is demonstrated by applying them both to the analysis of data obtained in the characterization of a Nb–Ti standard reference material supplied by NBS. Data taken at temperatures of 4.24 and 2.21 K are used to illustrate that the three physical parameters obey general scaling laws and to outline the physical interpretation which is derived for the empirical parameters. The validity of flux flow in high current density materials being characterized by defect motion with the flux line lattice is demonstrated.

Keywords: superconductors; Nb–Ti; critical currents; mathematical models

This Paper presents a comparison between the three parameter fit (3-P-F) the authors have considered before[1]

$$E = R_{IL} \int_b^I (I - I_i) f\left(\beta\left(\frac{I_i - \bar{I}_c}{\bar{I}_c}\right)\right) \cdot dI_i \qquad (1)$$

where:

E = electric field along the superconductor;

I = transport current;

f = normal density function;

$\bar{I}_c$ = mean critical current;

R_{IL} = interaction length resistance;

β = synchronization constant (a measure of the spread); and

b = constant†

and the empirical 2-P law which can be written in the form[2–4]‡

$$E = \alpha I^n \qquad (2)$$

(The parameters α and n are termed the alpha parameter and the index.)

The first section addresses a brief physical interpretation of the 3-P fit. It demonstrates the compatibility between this functional form and the empirical law. The limiting forms of the E–I characteristic are derived in the ranges of high, intermediate and low currents. The section is completed with the derivation of simple relations relating the empirical parameters of the 2-P law to the physical parameters of the 3-P fit.

In the second section, data are presented on a Nb–Ti wire which has been adopted by NBS[5] as their standard reference material**. The analysis of data presented previously, at 4.24 K is extended to include characterization using the empirical law and the physical interpretation of the empirical parameters explicitly outlined. Additional data generated at 2.21 K are presented and are again interpreted in terms of the 2-P and 3-P fits. The scaling laws governing the three physical parameters observed for Nb_3Sn throughout its entire superconducting phase are shown to hold for this Nb–Ti.

Finally, the theoretical and experimental problems associated with developing a more complete characterization of superconducting materials is discussed.

Three parameter fit

A detailed derivation of the 3-P-F has been given elsewhere[6]. The basic physical concepts are as follows.

It has long been appreciated that in defect-free systems, an ohmic-type law characterizes the state of flux flow of the form

$$E = R_{fL}(I - I_c) \qquad (3)$$

*Present address: Applied Superconductivity Centre, University of Wisconsin-Madison, 917 Engineering Research Building, 1500 Johnson Drive, Madison, WI 53706, USA

†In Reference 1, the constant b in Equation (1) was taken to be equal to zero since clearly negative currents (i.e. $I_i < 0$) are non-physical. However, in this work we shall take $b = -\infty$ for mathematical tractability, assuming that β and I_c are such that the contribution to the integral for $I_i < 0$ is negligible. Physically this is equivalent to assuming that over the E–I range of interest, the effect due to the low current tails of the distribution for $I_i < 0$ can be ignored. For the data presented it will be seen that this is indeed appropriate

‡The E–I forms for Equations (1) and (2) are used since these forms explicitly demonstrate that for the purposes of comparison there is a redundancy in the parameter: area of superconductor

**It should be noted that one of the samples of ≈2.2 m, commercially available from NBS, was not used. Instead a longer length (≈6 m) from the same batch of material was used

0011-2275/87/110608-09 $03.00

where: R_{fL} = flux flow length resistance; and I_c = critical current.

For highly inhomogeneous materials[††], one must consider the variation of I_c along the length of the material. In the simplest case, a distribution in critical currents is considered and the resultant E–I characteristic is merely a superposition of the ohmic-type relations given by Equation (3). Thus

$$E = R_{IL} \int_{-\infty}^{I} (I - I_i) f(I_i) dI_i \tag{4}$$

and

$$f(I) = \frac{1}{R_{IL}} \cdot \frac{\partial^2 E}{\partial I^2} \tag{5}$$

where: I_i = local critical current in a given region; and R_{fL} has been replaced by R_{IL} (=the interaction length resistance) since, as will be shown, R_{IL} is not simply the flux flow resistance.

The functional forms of Equations (4) and (5) have been presented before. The function $f(I)$ has been interpreted as defining the interaction between flux flow and stationary flux – a unique single value for I_c was assumed[7]. However, in the present interpretation, this interaction is not introduced. Following Jones *et al.*[8], the superconducting material is considered to be divided up into regions of unique and different critical current. The junction $f(I)$ characterizes the distribution in critical currents.

It has been shown experimentally that $f(I)$ approximates well to a normal density function[1]. This is in agreement with the central limit theorem which predicts this functional form, since superconductors consist of a large number of different sources of inhomogeneity[9]. Similarly, this normal density function can be justified in the limit of a great number of defects acting jointly on each vortex and contributing additively to the total pinning drag force[10]. More recently, in a detailed deconvolution of the E–I characteristic, the essentially Gaussian nature of the distribution has been verified and some of the deviations from the normal density function have been measured[11].

The limiting functional forms of the E–I characteristic are considered below. Equation (4) can be rewritten

$$E = R_{IL} \int_{-\infty}^{I} (I - I_i) \frac{1}{(2\pi)^{\frac{1}{2}}} \cdot \frac{\beta}{\bar{I}_c} \cdot \exp\left[-\frac{1}{2} \left(\beta \left(\frac{I_i - \bar{I}_c}{\bar{I}_c} \right) \right)^2 \right] \cdot dI_i \tag{6}$$

Integrating by parts

$$E = R_{IL} \left\{ (I - \bar{I}_c) \int_{-\infty}^{I} \frac{1}{(2\pi)^{\frac{1}{2}}} \cdot \frac{\beta}{\bar{I}_c} \cdot \exp\left[-\frac{1}{2} \left(\beta \left(\frac{I_i - \bar{I}_c}{\bar{I}_c} \right) \right)^2 \right] \cdot dI_i + \frac{1}{(2\pi)^{\frac{1}{2}}} \cdot \frac{\bar{I}_c}{\beta} \cdot \exp\left[-\frac{1}{2} \left(\beta \left(\frac{I - \bar{I}_c}{\bar{I}_c} \right) \right)^2 \right] \right\} \tag{7}$$

[††]This description of the material effectively defines the dominant mechanism for loss due to viscous flux flow [i.e. Equation (2)]. Clearly, in general, other mechanisms such as flux creep will need to be incorporated. However, it is demonstrated that the results derived for this specific case are sufficient to explain the data presented in this work

(1) For $I \to +\infty$

This is the high voltage limit occurring in the high current tails of the distribution function. The second term in Equation (7) tends to zero. Substituting the normalization condition

$$\int_{-\infty}^{\infty} \frac{1}{(2\pi)^{\frac{1}{2}}} \cdot \frac{\beta}{\bar{I}_c} \exp\left\{ -\frac{1}{2} \left(\beta \left(\frac{I_i - \bar{I}_c}{\bar{I}_c} \right) \right)^2 \right\} \cdot dI_i = 1 \tag{8}$$

we find

$$\lim_{I \to +\infty} E = R_{IL}(I - \bar{I}_c) \tag{9}$$

(2) For $I = \bar{I}_c$

This is the intermediate current limit where the greatest proportion of regions are at criticality, changing from regions of stationary flux to regions of flux flow.

If we consider the integral (S) in Equation (7) where

$$\lim_{I \to \bar{I}_c} S = \lim_{I \approx \bar{I}_c} \int_{-\infty}^{I} \frac{1}{(2\pi)^{\frac{1}{2}}} \cdot \frac{\beta}{\bar{I}_c} \cdot \exp\left[-\frac{1}{2} \left(\beta \left(\frac{I_i - \bar{I}_c}{\bar{I}_c} \right) \right)^2 \right] dI_i \tag{10}$$

Then, by letting $x = \beta\left(\frac{I_i - \bar{I}_c}{\bar{I}_c} \right)$, $\gamma = I/\bar{I}_c$ and using standard expansions

$$\begin{aligned} \lim_{I = \bar{I}_c} S &= \int_{-\infty}^{0} \frac{1}{(2\pi)^{\frac{1}{2}}} \cdot \exp -\frac{1}{2} x^2 \cdot dx \\ &\quad + \int_{0}^{(\gamma - 1)\beta} \frac{1}{(2\pi)^{\frac{1}{2}}} \cdot \exp -\frac{1}{2} x^2 \cdot dx \\ &= \frac{1}{2} + \int_{0}^{(\gamma - 1)\beta} \frac{1}{(2\pi)^{\frac{1}{2}}} \cdot \left(1 - \frac{1}{2} x^2 + \cdots \right) dx \\ &= \frac{1}{2} + \frac{\beta}{(2\pi)^{\frac{1}{2}}} \cdot (\gamma - 1) + 0[(\gamma - 1)^3] \end{aligned} \tag{11}$$

$$\Rightarrow \lim_{I \approx \bar{I}_c} E = R_{IL} \left\{ (I - \bar{I}_c) \left[\frac{1}{2} + \frac{\beta}{(2\pi)^{\frac{1}{2}}} \cdot \left(\frac{I - \bar{I}_c}{\bar{I}_c} \right) \right] + \frac{\bar{I}_c}{\beta} \cdot \frac{1}{(2\pi)^{\frac{1}{2}}} \cdot \left[1 - \frac{1}{2} \left(\beta \left(\frac{I - \bar{I}_c}{\bar{I}_c} \right) \right)^2 \right] + 0[(\gamma - 1)^3] \right\} \tag{12}$$

Therefore

$$\lim_{I \approx \bar{I}_c} E = R_{IL} \frac{\bar{I}_c}{\beta (2\pi)^{\frac{1}{2}}} \tag{13}$$

(3) For $x^2 = \left| \beta \left(\frac{I_i - \bar{I}_c}{\bar{I}_c} \right) \right|^2 \gg 1$

This is the condition for the low voltage limit occurring in the low current tails of the distribution function, which can be considered as appropriate for $I \to 0$.

Using an expansion for the integral S[12] we find

$$\lim_{|x|^2 \gg 1} S = \frac{1}{(2\pi)^{\frac{1}{2}}} \cdot \exp -\frac{1}{2} x^2 \left[-\frac{1}{x} + \frac{1}{x^3} - \cdots \right] \tag{14}$$

Substituting into Equation (7)

$$E = R_{IL}\left\{(I-\bar{I}_c)\left(\frac{1}{(2\pi)^{\frac{1}{2}}}\right.\right.$$
$$\cdot\exp\left[-\frac{1}{2}\left(\beta\left(\frac{I-\bar{I}_c}{\bar{I}_c}\right)\right)^2\right]\left)\left(\frac{-\bar{I}_c}{(I-\bar{I}_c)\beta}+\frac{\bar{I}_c^3}{(I-\bar{I}_c)^3\beta^3}\right)\right.$$
$$\left.+\frac{\bar{I}_c}{\beta}\cdot\frac{1}{(2\pi)^{\frac{1}{2}}}\cdot\exp\left[-\frac{1}{2}\left(\beta\left(\frac{I-\bar{I}_c}{\bar{I}_c}\right)\right)^2\right]\right\} \quad (15)$$

Therefore

$$\lim_{|x|^2\gg 1} E = R_{IL}\left\{\frac{\bar{I}_c^3}{(I-\bar{I}_c)^2\beta^3}\cdot\frac{1}{(2\pi)^{\frac{1}{2}}}\right.$$
$$\left.\cdot\exp\left[-\frac{1}{2}\left(\left(\frac{I-\bar{I}_c}{\bar{I}_c}\right)\beta\right)^2\right]\right\} \quad (16)$$

Thus we have the expressions for the limiting functional forms of the E–I characteristic assuming a normal density function for the distribution in critical currents [Equations (9), (13) and (16)].

In *Figures 1* and *2*, general E–I characteristics have been plotted for two values of I_c (150 and 300 A) for different values of β. However, the value of R_{IL} has been left as a free parameter since it has been demonstrated for Nb–Ti and Nb_3Sn that R_{IL} is typically five orders of magnitude less than the normal resistivity of the respective materials[6]. The figures explicitly demonstrate the functional form of the E–I characteristics. In *Figures 3* and *4*, the functional form of these E–I characteristics have been replotted on a log–log scale. It is clear that the 3-P functional form predicts that the empirical law will hold to a good approximation in the low current tail over a number of decades of electric field[13].

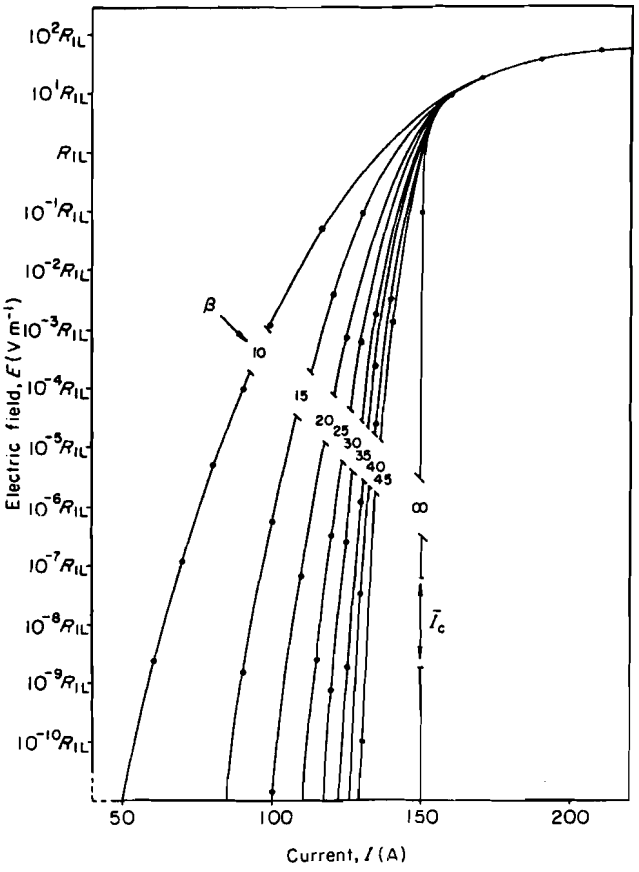

Figure 1 General E–I characteristic on a log–linear scale, assuming a normal density function for the critical currents, where R_{IL} is a free parameter (Ω m^{-1}), I_c = 150 A and β (the synchronization constant) is a variable

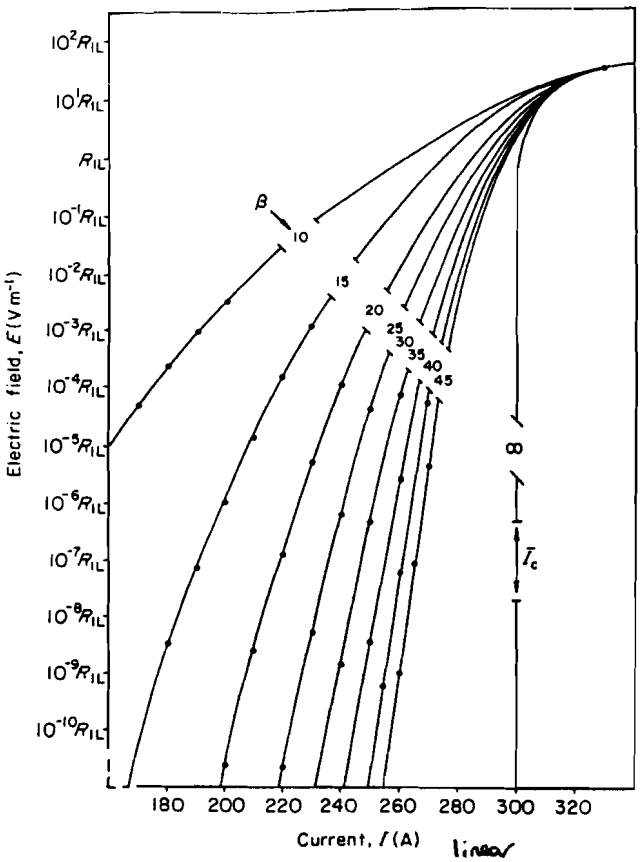

Figure 2 General E–I characteristic on a log–log scale, assuming a normal density function for the critical currents, where R_{IL} is a free parameter (Ω m^{-1}), I_c = 300 A and β (the synchronization constant) is a variable

This section concludes using the equations derived, by determining the relations between the empirical constants α and n, and the physical parameters R_{IL}, I_c and β. In the high current limit [i.e. limit (1)] by equating Equation (9) to Equation (2) it is concluded that $\lim_{I\to\infty} \alpha = R_{IL}$ and $\lim_{I\to\infty} n = 1$. In the low current limit [i.e. limit (3)], it is clear from *Figures 2* and *4* that the convex nature of the curves implies $\lim_{|x|^2\gg 1} n \to \infty$, and the insensitivity of the index n with current that is mentioned above implies $\lim_{|x|^2\ll 1} \alpha \to 0$. In the intermediate current range [i.e. limit (2)] which is of most interest in the analysis of the data presented, we have from Equation (2)

$$\lim_{I\approx\bar{I}_c} E = R_{IL}\left\{\frac{\bar{I}_c}{\beta(2\pi)^{\frac{1}{2}}}+\frac{1}{2}(I-\bar{I}_c)+0((\gamma-1)^2)\right\} \quad (18)$$

$$\lim_{I\approx\bar{I}_c} \frac{\partial E}{\partial I} = R_{IL}\left\{\frac{1}{2}+\frac{2\beta}{(2\pi)^{\frac{1}{2}}}\cdot\left(\frac{I-\bar{I}_c}{\bar{I}_c}\right)+0((\gamma-1))^2\right\} \quad (19)$$

Therefore

$$\lim_{I\approx\bar{I}_c} n = \beta\left(\frac{\pi}{2}\right)^{\frac{1}{2}} \quad (20)$$

This equation can be rewritten in terms of the standard

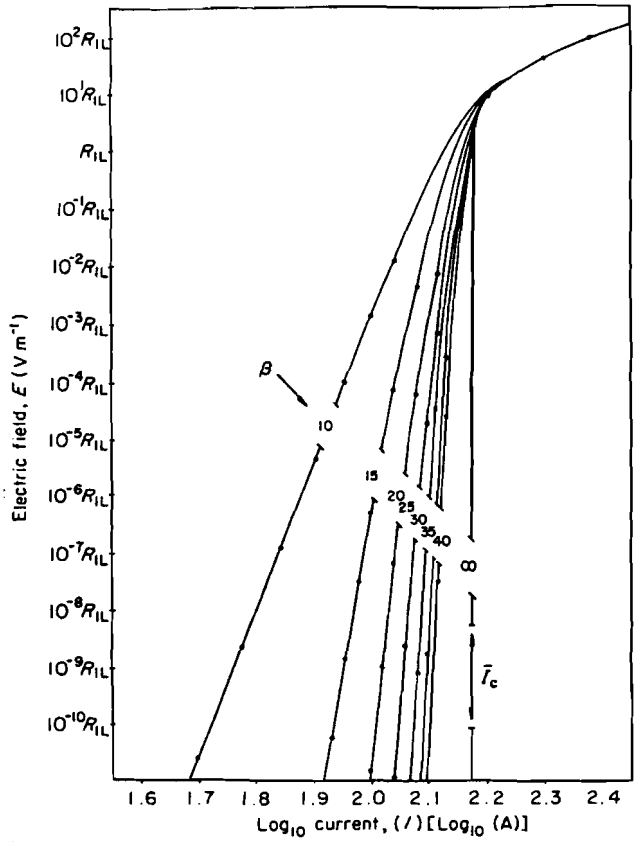

Figure 3 General *E–I* characteristic on a log–log scale, assuming a normal density function for the critical currents, where R_{IL} is a free parameter ($\Omega\,m^{-1}$), $I_c = 150$ A and β (the synchronization constant) is a variable

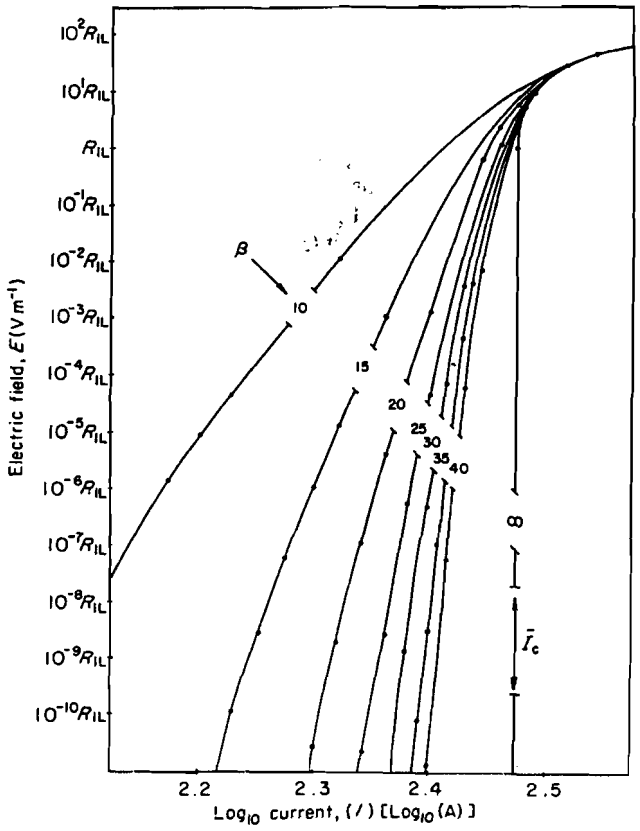

Figure 4 General *E–I* characteristic on a log–log scale, assuming a normal density function for the critical currents, where R_{IL} is a free parameter ($\Omega\,m^{-1}$), $I_c = 300$ A and β (the synchronization constant) is a variable

deviation of the critical current distribution, σ, where

$$\sigma = \frac{\bar{I}_c}{\beta} = \frac{\bar{I}_c}{n} \cdot \left(\frac{\pi}{2}\right)^{\frac{1}{2}} \tag{21}$$

From Equation (19) we have

$$\lim_{I \approx \bar{I}_c} \frac{\partial E}{\partial I} = \frac{1}{2} R_{IL} = \alpha n I^{n-1} \tag{22}$$

Therefore

$$\lim_{I \approx \bar{I}_c} \alpha = \left(\frac{1}{2\pi}\right)^{\frac{1}{2}} \cdot \frac{R_{IL}}{\beta[\bar{I}_c^{[\beta(\frac{\pi}{2})^{\frac{1}{2}}-1]}]} \tag{23}$$

It is pertinent to note that Equation (22) may be rewritten

$$R_{IL} = 2nE_{I=\bar{I}_c}(I)/\bar{I}_c \tag{24}$$

Thus, from Equations (20) and (23) we have the empirical parameters in terms of the physical parameters. This allows interpretation of the field and temperature dependence of the index n and the alpha parameter. This will be explicitly outlined using data from the SRM Nb–Ti wire in the next section.

Data on the SRM Nb–Ti wire

Experimental procedure

The equipment and experimental techniques for generating the *E–I* data have been detailed by the authors in the preceding paper on this material[14]. The recommendations outlined by NBS for measuring the electric field–current transitions of this material have been closely followed to obtain these data. At each fixed temperature, a direct current was slowly increased through the superconducting specimen and the voltage generated across the potential taps measured. The ramp rate for the sample current was chosen so that within experimental accuracy, the *E–I* transition was reversible for I increasing and I decreasing. A hard copy was produced of the voltage *versus* current.

The self-field effects, which are only significant below 3 T were eliminated by taking two traces for opposite direction of current flow. The mean value of current at each voltage was used to define the zero self-field *E–I* characteristic. No strain effects were observed.

During measurement the sample lay in intimate thermal contact with the helium bath. The temperature was stabilized by monitoring a manometer connected by a static line to the pumped dewar. Standard vapour pressure curves were used to calibrate the temperature at 4.24 and 2.21 K.

The hard copy *E–I* characteristics were digitized between 10 and 50 $\mu V\,m^{-1}$ at 5 $\mu V\,m^{-1}$ intervals. Above $B_{c2}(T)$ the resistance of the sample and sample holder was measured and found to be field independent (the contribution of the superconductor in the normal state is negligible). At each voltage measured, the appropriate current being shunted through this parallel ohmic path was subtracted and the corrected current through the superconductor alone obtained as a function of voltage.

A full analysis of the errors in measurements generated using these techniques has been presented elsewhere[14]. This analysis suggests that the errors in the data can be quoted in terms of uncertainty in temperature of ± 0.05 K.

Results

The analysis of the corrected E–I characteristics in terms of both the empirical 2-P law and the 3-P fit is considered below. The universality of the pinning force in agreement with the Fietz–Webb[15] scaling law is demonstrated as well as the universality of the synchronization constant and the interaction resistance as has been found for Nb_3Sn[6].

For mathematical tractability, the normal distribution function intrinsic to the 3-P fit can be rewritten to a good approximation over the range of the distribution that is sampled by

$$\phi(I) = \int_{-\infty}^{I} \frac{1}{(2\pi)^{\frac{1}{2}}} \cdot \frac{\beta}{\bar{I}_c} \cdot \exp\left[-\frac{1}{2}\left(\beta\left(\frac{I_i - \bar{I}_c}{\bar{I}_c}\right)\right)^2\right] \cdot dI_i$$

$$= \frac{1}{2}\left[1 + \tanh\left(0.84\beta\left(\frac{I - \bar{I}_c}{\bar{I}_c}\right)\right)\right] \quad (25)$$

Thus the raw data was fitted to the following two equations over the range 10–50 $\mu V\,m^{-1}$

$$E = R_{IL}\left\{(I - \bar{I}_c)\cdot\frac{1}{2}\left[1 + \tanh\left(0.84\beta\left(\frac{I - \bar{I}_c}{\bar{I}_c}\right)\right)\right] + \frac{1}{(2\pi)^{\frac{1}{2}}}\cdot\frac{\bar{I}_c}{\beta}\exp\left[-\frac{1}{2}\left(\beta\left(\frac{I - \bar{I}_c}{\bar{I}_c}\right)\right)^2\right]\right\} \quad (26)$$

and

$$E = \alpha I^n \quad (27)$$

These parameters are considered in turn below.

Mean critical current. In *Figure 5*, the mean value of the critical current is presented as a function of field at 4.24 and 2.21 K. The difference between the mean critical current and the critical current at 30 $\mu V\,m^{-1}$ for this particular Nb–Ti material is less than 1 A (i.e. less than the size of the symbol in *Figure 5*). It is of interest to note that the functional form of the pinning force and the characteristic significant deviation from linearity in low field is compatible with the model that predicts that the critical current of Nb–Ti is determined by the shearing of defects in the F-L-L past point pinning centres[16].

In *Figure 6*, the critical current data has been replotted as the reduced pinning force *versus* the reduced magnetic field. The universality of these data in agreement with the Fietz–Webb Scaling Law is explicitly demonstrated.

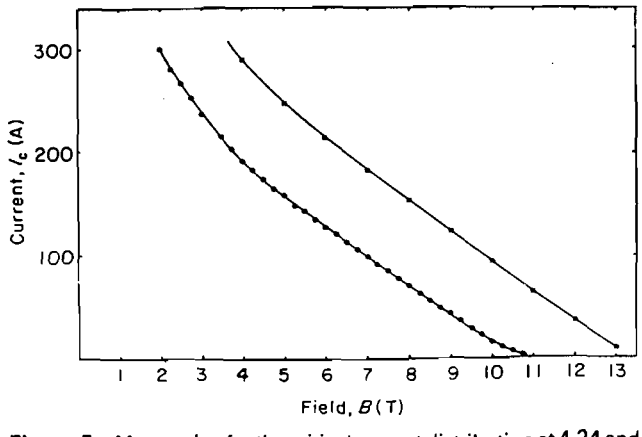

Figure 5 Mean value for the critical current distribution at 4.24 and 2.21 K as a function of field for the Nb–Ti SRM. ●, 4.24 K; ■, 2.21 K

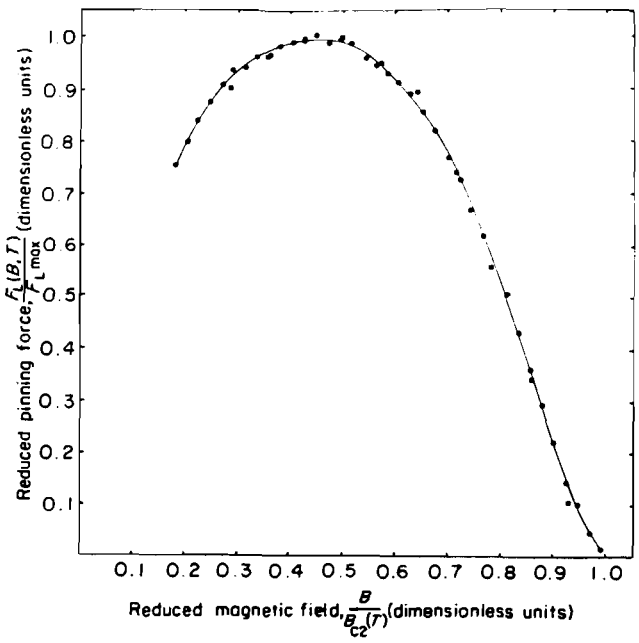

Figure 6 Reduced pinning force *versus* reduced magnetic field at: ●, 4.24 K; and ■, 2.21 K for the Nb–Ti SRM

Synchronization constant β/Index n. In *Figure 7* the synchronization constant β is plotted as a function of field at 4.24 and 2.21 K. The parameter β_F is the value obtained from the full 3-P fit using Equation (23). The parameter β_E is defined by

$$\beta_E = n\left(\frac{2}{\pi}\right)^{\frac{1}{2}} \quad (28)$$

in accordance with Equation (20). In agreement with the algebraic manipulations in the three parameter fit section, we have

$$\beta_E(\bar{I}_c) = \beta_F(\bar{I}_c) \quad (29)$$

This equality has been observed experimentally by Warnes and Larbalestier. Their data can be expressed by $\beta_E = (1.2 \pm 0.2)\beta_F$*.

The difference between β_F and β_E that is observed in *Figure 7* occurs since the equality in Equation (29) only holds rigorously at I_c. In practice, these parameters have been determined by fits taken over a range about I_c.

It is shown in any elementary statistical text that[12]

$$\frac{1}{\beta_F^2} = \frac{(I_i^2) - (\bar{I}_c)^2}{(\bar{I}_c)^2} \quad (30)$$

Thus we now have a physical interpretation of the index n through the synchronization constant, β.

In *Figure 8*, the universality of the synchronization constant that has been found for 1.5 T $\leqslant B \leqslant$ 15 T and

*The data in the paper referred to (Reference 12) has been presented in terms of I(FWHM) where FWHM = full width half maximum. Since

$$\delta I(\text{FWHM}) = 2\sigma(\log_e 4)^{1/2} \quad (37)$$

From Equation (21)

$$\frac{\bar{I}_c}{\delta\bar{I}_c(\text{FWHM})} = \left[\frac{1}{(\log_e 4)2\pi}\right]^{1/2} \cdot n \quad (38)$$

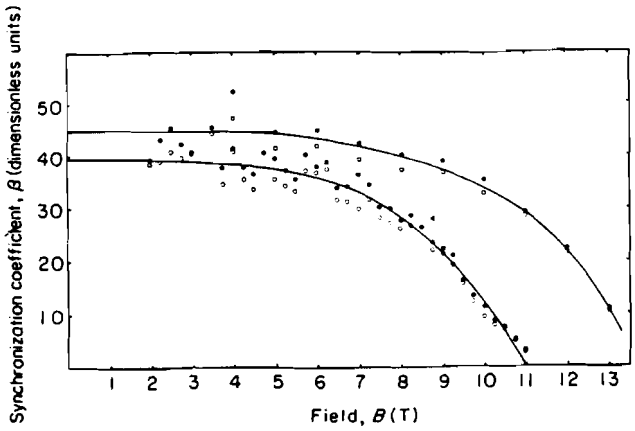

Figure 7 Synchronization constant as a function of field at 4.24 and 2.21 K for the Nb–Ti SRM. ■, β_E(2.21 K); ●, β_E(4.24 K); □, β_F(2.21 K); ○, β_F(4.24 K)

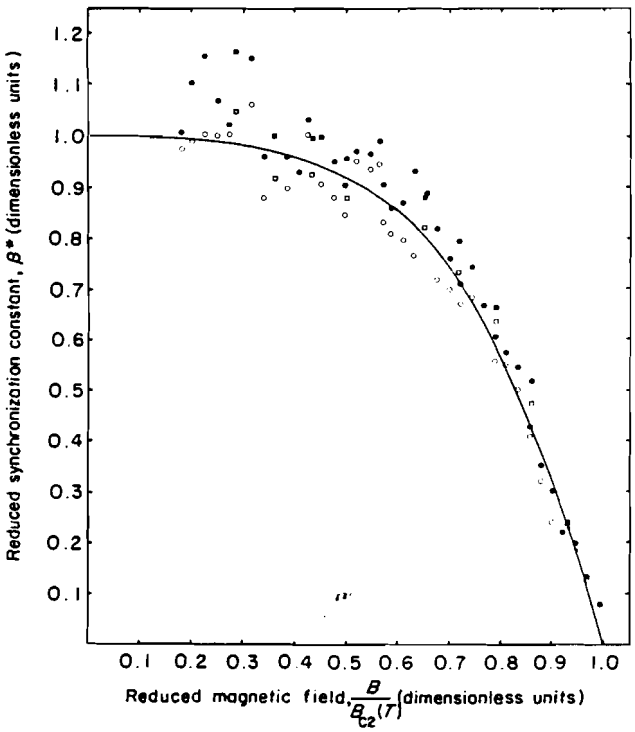

Figure 8 Reduced synchronization constant *versus* reduced magnetic field at 4.24 and 2.21 K for the Nb–Ti SRM. Symbols as for *Figure 7*

$2.5\,\mathrm{K} < T \leqslant T_c$ for Nb_3Sn is demonstrated for this particular Nb–Ti wire. The reduced synchronization constant, β^*, is defined by

$$\beta^* = \frac{\beta(B, T)}{\beta(0, T)} \tag{31}$$

where $\beta(0, 4.24\,\mathrm{K}) = 39.5$ and $\beta(0, 2.21\,\mathrm{K}) = 45.0$. From Equation (30) it can be seen that insofar as the synchronization constant, or equivalently the index n, is independent of reduced field (for $b < 0.4$) but is a function of temperature, the different critical currents that characterize this Nb–Ti material are given (within this range) by

$$I_{ci} = f_i(T)g(b) \tag{32}$$

This equation implies that the component regions of different I_{ci} have the same reduced field dependence but have different temperature dependences. More generally it has been demonstrated that the universality of β demonstrates that the component regions of the distribution obey different scaling laws which are all of the general Fietz–Webb type. The field and temperature dependence of a material's universal synchronization curve characterizes the different functional forms of $f(T)$ and $g(b)$ that are found in these regions throughout the material[6].

Interaction length resistance/alpha parameter. In *Figure 9* the interaction length resistance is plotted as a function of field at 4.24 and 2.21 K. The salient feature of these data is that to within experimental accuracy the interaction length resistance is a linear function of field through the origin at low fields as has been found for the high current material Nb_3Sn by the authors and for many defect-free (low current) Type II superconductors[17,18]. The deviation at the lowest field in the data (at 2 T) from the idealized straight-line can be attributed to heating causing a temperature increase of 0.05 K during the transition.

The universality of this parameter is demonstrated in *Figure 10* where the interaction coefficient, α^*, is plotted as a function of reduced field. The interaction coefficient, α^*, is defined by

$$\alpha^* = \frac{R_{IL}(B, T)}{B_{c2}(T) \cdot \left(\lim_{B \to 0} \dfrac{\partial R_{IL}(B, T)}{\partial B} \right)} \tag{33}$$

which normalizes $R_{IL}(B, T)$ using the idealized straight-line through the origin.

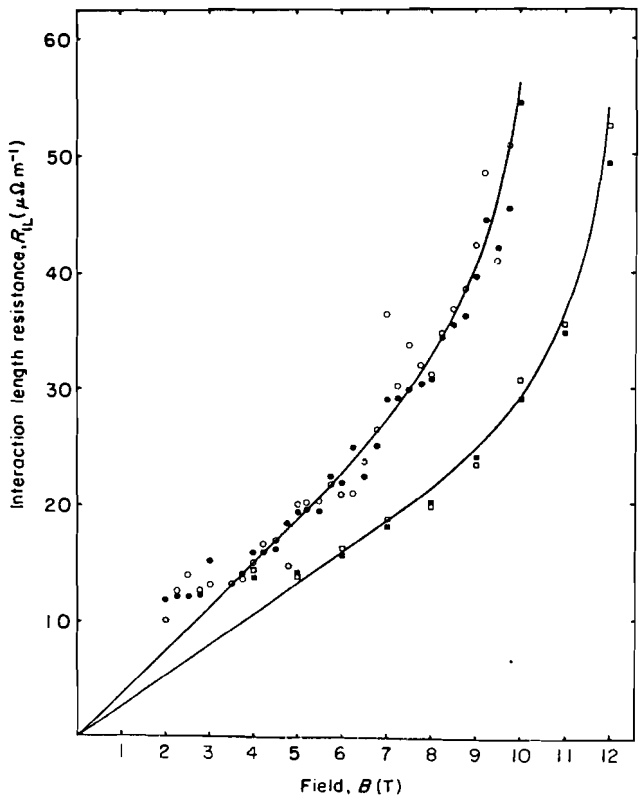

Figure 9 Interaction length resistance of the Nb–Ti SRM *versus* magnetic field at 4.24 and 2.21 K. ■, R_{IEL}(2.21 K); ●, R_{IEL}(4.24 K); □, R_{IL}(2.21 K); ○, R_{IL}(4.24 K)

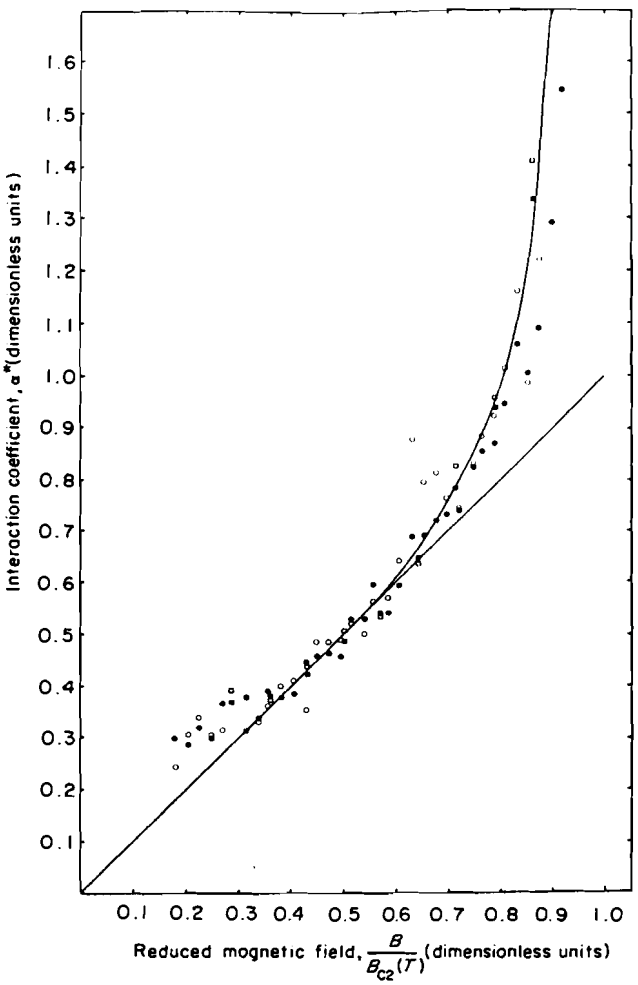

Figure 10 Interaction coefficient *versus* reduced magnetic field at 4.24 and 2.21 K for the Nb–Ti SRM. ■, α_E(2.21 K); ●, α_E(4.24 K); □, α_F(2.21 K); ○, α_F(4.24 K)

Thus *Figure 10* shows

$$R_{IL}(B, T) = R_{IL}(0) \cdot b \cdot K(b) \cdot L(T/T_c) \quad (34)$$

where:

$b = B/B_{c2}(T)$;

$\lim_{B \to 0} K(b) = 1$;

$\lim_{T \to 0} L(T/T_c) = 1$; and

$R_{IL}(0)$ = a constant characteristic length resistance of the material in the flux flow state.

It is interesting to note that for this Nb–Ti, $L(T) = 1/(1 - T/T_c)^{1/3 \pm 2/3}$. By extrapolating to $T = 0$

$$R_{IL}(0) = B_{c2}(0) \cdot \lim_{B \to 0} \frac{\partial R_{IL}(B, 0)}{\partial B} = 33.8\ \mu\Omega\ \mathrm{m}^{-1}$$

Or equivalently for this wire

$$\rho_I(0) = B_{c2}(0) \lim_{B \to 0} \cdot \frac{\partial \rho_I(B, T)}{\partial B} = 2.5 \times 10^{-4}\ \mu\Omega\,\mathrm{cm}$$

where ρ_I is the interaction resistivity.

A possible model of the interaction length resistance can be made in terms of it being characteristic of random distribution of inhomogeneities[9]. In this case the supercurrent increases through the superconductor until criticality just before flux flow is about to occur. Beyond criticality, because of the superconductor's high differential resistivity, any further increase in currents is shunted through the low resistivity copper matrix. In this case R_{IL} becomes simply the matrix resistivity and the field dependence is due merely to the magnetoresistance of the high resistivity ratio copper necessary for stability in this wire. However, this model is not appropriate here since although it could be argued that the field dependence in *Figure 9* is the magnetoresistance of the copper matrix, one would expect R_{IL} to be independent of temperature, which is clearly not the case. The data on Nb_3Sn presented by the authors shows R_{IL} changing by an order of magnitude at 2 T between 2 and 10 K. The very low value for the interaction resistivity found above demonstrates that in the flux flow state when most of the component regions in the normal density distribution of critical currents are above criticality, only a small fraction of the total fluxons present are in motion. This has been interpreted by the authors as direct experimental evidence that flux flow is characterized by the motion of defects within the flux line lattice. This is analogous to the role of defects in real crystals reducing the critical stress by many orders of magnitude from that of the ideal crystal. In conclusion: the function f describes the distribution in critical currents associated with the different defects within the flux line lattice; R_{IL} is a field and temperature dependent length resistance, characterizing the superconductor when all the defects within the flux line lattice are in motion.

In *Figure 11* the length resistance of Nb–Ti (i.e. with the matrix etched off) is plotted as a function of temperature. The standard Kohler law predicts there is no intrinsic field dependence of the normal state resistivity for this Nb–Ti. This figure demonstrates that in the normal state above T_c the length resistance R_{NL} is given by

$$R_{NL} = 6.97\ \Omega\ \mathrm{m}^{-1} \pm 0.1\ \Omega\,\mathrm{m}^{-1}$$

or equivalently

$$\rho_N = 52\ \mu\Omega\,\mathrm{cm} \pm 1\ \mu\Omega\,\mathrm{cm}$$

Theoretical and experimental analyses of defect-free Type II superconductors assert that above criticality, in the flux

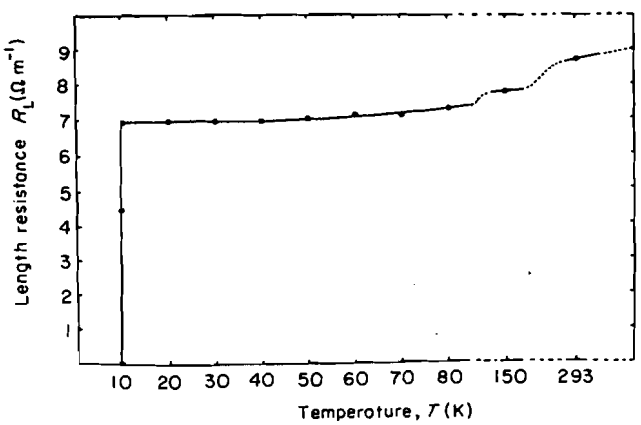

Figure 11 Length resistance of the Nb–Ti SRM as a function of temperature

flow state

$$\lim_{B \to 0} R_{fL}(B, T) = \frac{B}{B_{c2}(0)} \cdot R_{NL} \quad (35)$$

where R_{fL} is defined in Equation (3).

It is important to note that Equation (35) is derived for a homogeneous system with randomly distributed point scattering centres. Certainly the data here demonstrates that the interaction resistance is some five orders of magnitude less than the flow resistance, although the linearity in fields common to both seems highly significant.

It is certainly clear that more theoretical input is required to generalize Equation (35) from its appropriate idealized system to more complex systems such as Nb–Ti. Equally, more measurements of the flux flow resistivity and interaction resistivity are required to characterize the functional form of, and relationship between, these two parameters.

In *Figures 9* and *10*, the empirical derivation of the interaction length resistance, R_{IEL}, is also presented. The 3-P fits show that for this particular Nb–Ti material, I_c is found at a voltage criterion of $\approx 30\,\mu V\,m^{-1}$. If we use this electric field criterion to arbitrarily define I_c, then either using the alpha parameter directly through Equation (23) or equivalently through Equation (24) we have

$$R_{IEL} = 2nE_{I=I_c}\frac{(I)}{I_c} = \frac{2n30\,\mu V\,m^{-1}}{\lim_{E=30\mu Vm^{-1}} \cdot I} \quad (36)$$

The good agreement between R_{IEL} and R_{IL} can be seen in these two figures. It is interesting to note that for two high current samples, Nb_3Sn and Nb–Ti, I_c has been found at a fixed electric field criterion throughout the field temperature range (≈ 50 and $\approx 30\,\mu V\,m^{-1}$, respectively). However, more data will be required to decide whether Equation (22) can be generally used as a technical tool to obtain an order of magnitude estimate of the interaction length resistance using the empirical 2-P law without having to embark on the significant input involved in the full 3-P fit.

More complete characterization of superconducting materials

In this final section, the theoretical and experimental problems associated with developing a more complete characterization of superconducting materials and in particular the field and temperature dependence of their distribution function is discussed.

Consider an idealized case consisting of a highly stoichiometric material which has a normal density function distribution of critical currents. It is clear that the first three regions of the E–I characteristic can be described as follows: 1, an initial low voltage region where there is very little flux flow and the conductivity is essentially infinite; 2, an intermediate region of high curvature in the characteristic occurring over a range I_c/β (flux flow is just beginning in many regions); and 3, a linear high voltage region where $\partial E/\partial I = R_{IL}$ and where this linearity extrapolates through I_c. (At higher transport currents there are other regions characterized, for example, by the motion of all unpinned fluxons or the bulk motion of all fluxons.) Necessarily, in order to uniquely associate the function derived in deconvolution with the distribution of critical currents intrinsic to the sample [using Equation (5)], it is clear that the ohmic-type relation [Equation (3)] must hold in all regions where I_i is less than I. It has been shown that this linear relation will break down at large currents and electric fields since: I_i is not independent of transport current at high currents and in particular[19] $\lim_{I \to \infty} I_i = 0$; and for very high current density materials at very high electric fields there is significant power dissipation which will increase R_{ii}. These inevitable non-linear effects will cause a non-zero value of $\partial^2 E/\partial I^2$ beyond the linear region which is not attributable to the intrinsic distribution in critical currents. Physically this argument can be seen as follows: the E–I characteristic can be seen to be a superposition of 'ohmic-type' characteristics defined by Equation (3). It is not possible when deconvoluting the E–I characteristic to distinguish non-linearity in this equation from intrinsic variations in the distribution function unless the non-linear terms can either be corrected for or shown to be insignificant.

If we now consider a more extreme case, where non-linearity has started to occur before all regions are above their local critical current, it is clear that there will be no linear region in the E–I characteristic. One of the fundamental difficulties in the analysis of these systems will be due to the impossibility of proving a priori, from the E–I characteristic alone, when non-linearity becomes significant.

Certainly to address these questions comprehensively accurate measurement of the double-differential of the E–J characteristic will be required. Recently Warnes and Larbalestier have been addressing this. It would be of interest to complement their approach by measuring this quantity (and hence the distribution function) directly using, for example, a pair of coupled circuits, most importantly to test for the non-reversibility of the distribution function (which is to be expected to at least some degree since critical current density is not a fundamental thermodynamic function), to reduce the time of analysis, and in order to investigate the non-linear effects discussed above.

Conclusions

1 Data has been generated characterizing a Nb–Ti SRM at 4.24 and 2.21 K.
2 The compatibility between the 2-P empirical law and the 3-P fit has been demonstrated.
3 The universality of R_{IL}, the interaction length resistance, and β, the synchronization constant, has been demonstrated for this particular Nb–Ti.
4 The interaction length resistance is a field and temperature dependent parameter characteristic of the superconductor. The E–I characteristic is characteristic of the bulk superconductor and not due to damaged regions along its length.
5 The universality of the β constant demands that the component regions of the superconductor obey different scaling laws which are all of the Fietz–Webb functional form.
6 A physical interpretation of the empirical index, n, has

been given through the equation

$$n = \beta\left(\frac{\pi}{2}\right)^{\frac{1}{2}} \tag{20}$$

or equivalently

$$\sigma = \frac{\bar{I}_c}{\beta} = \frac{\bar{I}_c}{n}\left(\frac{\pi}{2}\right)^{\frac{1}{2}} \tag{21}$$

7 An estimate of the interaction length resistivity can be made through the equation

$$R_{IL} = 2nE_{I=I_c}\frac{(I)}{\bar{I}_c} \tag{24}$$

The magnitude of this parameter demonstrates that the mechanism for flux flow is characterized by defect motion within the flux line lattice.

8 An outline of the more exacting measurements required for a more comprehensive understanding of high current superconductors and some of the associated analytical problems have been discussed.

Acknowledgements

The authors are grateful to Mr J. Cosier for his help during the production of the data for *Figure 11*, Dr W. Warnes and Professor D.C. Larbalestier for copies of their work prior to publication, Dr A.F. Clark for providing the Nb–Ti material, and Mr Alan Day and Miss Penny Jackson for their help in the preparation of this publication.

References

1 **Hampshire, D.P. and Jones, H.** Critical current of a NbTi reference material as a function of field and temperature *Proc Ninth Int Magnet Technology Conf* (Eds Marinucci, C. and Weymuth, P.) Swiss Institute of Nuclear Research, Villigen, Switzerland (1986) 531

2 **Walters, C.R.** Brookhaven Laboratory Informal Report, BNL 18929 (AADD 74-2) (1974) 30–31

3 **Wilson, M.N.** *Superconducting Magnets* Clarendon Press, Oxford, UK (1983) 236

4 **Garber, M., Sampson, W.B. and Tannenbaum, M.J.** *IEEE Trans Magn* (1983) **MAG-19** (1983) 720–723

5 **Goodrich, L.F., Vecchia, D.F., Pittmann, E.S., Ekin, J.W. and Clark, A.F.** Critical current measurements on a NbTi superconducting wire standard reference material, NBS Special Publication (1984)

6 **Hampshire, D.P. and Jones, H.** A detailed investigation of the *E-J* characteristic and the role of defect motion within the flux-line-lattice for high current density, high field superconducting compounds, with particular reference to data on Nb_3Sn throughout its entire field temperature phase space. *J Phys C* in press

7 **Baixeras, J. and Fournet, G.** Pertes par deplacement de vortex dans un supraconducteur de Type II *J Phys Chem Sol* (1967) **28** 1541

8 **Jones, R.G., Rhoderick, E.H. and Rose-Innes, H.C.** Non-linearity in the voltage-current characteristic of a Type II superconductor *Phys Lett* (1967) **24A6** 318

9 **Plummer, C.J.G. and Evetts, J.E.** Dependence of the shape of the resistive transition on composite inhomogeneity in multifilamentary wires, Paper MF-6, presented at the Applied Superconductivity Conference, Baltimore, USA (1986)

10 **Magradze, O.V., Matgushkina, L.V. and Shukman, V.A.** Vortex motion in Type II superconductors with controllable type defects *J Low Temp Phys* (1985) **55** 475

11 **Warnes, W.H. and Larbalestier, D.C.** Critical current distributions in superconducting composites *Cryogenics* (1986) **26** 643

12 **Feller, W.** *An Introduction to Probability Theory and its Applications* Wiley Publications (1957) 179

13 First presented by **Evetts, J.E.** High field superconductors, presented at a meeting at the Rutherford Laboratory (5–6 February 1986)

14 **Hampshire, D.P. and Jones, H.** A new apparatus for measuring the critical currents of hard Type II superconductive wires and tapes in high fields as a function of temperature throughout their superconducting phase *J. Phys E* (1987) **20** 516

15 **Fietz, D.A. and Webb, W.** Hysteresis in superconducting alloys – temperature and field dependence of dislocation pinning in niobium alloys *Phys Rev* (1969) **178** 657

16 **Hampshire, D.P.** The characterisation of high field superconducting alloys and compounds *DPhil Thesis* The Clarendon Laboratory, Oxford, UK (1985)

17 **Bardeen, J. and Stephen, M.J.** Theory of the motion or vortices in superconductors *Phys Rev* (1965) **140** A1197

18 **Takayama, T.** Flux flow resistivity of superconducting thin films *J Low Temp Phys* (1977) **27** 3

19 **Lowell, J.** The frictional force on a moving fluxon *J Phys C* (1970) **3** 717